Algebraic States in Continuum in $d > 1$ Dimensional Non-Hermitian Systems

Ao Yang,[1,2] Kai Zhang,[3] and Chen Fang[1,4,*]
[1]Beijing National Laboratory for Condensed Matter Physics, and Institute of Physics, Chinese Academy of Sciences, Beijing 100190, China
[2]University of Chinese Academy of Sciences, Beijing 100049, China
[3]Department of Physics, University of Michigan Ann Arbor, Ann Arbor, Michigan 48109, USA
[4]Kavli Institute for Theoretical Sciences, Chinese Academy of Sciences, Beijing 100190, China

(Received 24 July 2025; revised 23 January 2026; accepted 25 March 2026; published 17 April 2026)

We report the existence of algebraically localized eigenstates embedded within the continuum spectrum of 2D non-Hermitian systems with a single impurity. These modes, which we term algebraic states in continuum (AICs), decay algebraically as $1/|r|$ from the impurity site, and their energies lie within the bulk continuum spectrum under periodic boundary conditions. We analytically derive the threshold condition for the impurity strength required to generate such states. Remarkably, AICs are forbidden in Hermitian systems and in 1D non-Hermitian systems, making them unique to non-Hermitian systems in two and higher dimensions. To detect AICs, we introduce a local density of states as an experimental observable, which is readily accessible in photonic and acoustic platforms.

DOI: 10.1103/9dhm-k5kf

Introduction—The distinction between localized and extended states, which determines essential properties such as conductivity, is fundamental to understanding diverse phases of matter [1–3]. In Hermitian systems, localized states typically have discrete energies and are separated from the continuum of extended scattering states [4]. An exception to this rule is the bound state in the continuum (BIC), a localized state whose energy resides within the continuum spectrum. BICs in Hermitian systems are structurally fragile and typically require fine-tuning of system parameters. This fragility arises from the necessity for BICs to decouple from surrounding extended scattering states to remain localized. Such decoupling often relies on symmetry protection or interference-based mechanisms. For example, an odd-parity BIC can remain localized if the continuum states have even parity, preventing hybridization due to symmetry mismatch [5]. Moreover, BICs in Hermitian systems exhibit exponential localization in arbitrary space dimensions. These limitations and characteristics motivate us to investigate BICs in non-Hermitian systems [6–20] through the following questions: (i) Is there a universal mechanism for the emergence of BICs in non-Hermitian systems that does not rely on symmetry protection or fine-tuning? (ii) What is the localization behavior for such BICs in non-Hermitian systems?.

The questions above are both reasonable and compelling, given the fundamental differences in two key aspects between Hermitian and non-Hermitian systems: spectral structure and wave function localization. Unlike Hermitian systems, where the energy spectrum lies along the real-energy axis, non-Hermitian systems typically feature complex energy eigenvalues that can span a finite area in the complex plane [21]. This results in a fundamentally distinct spectral structure and density of states, beyond the constraints of Hermitian systems. Moreover, non-Hermitian systems often exhibit the non-Hermitian skin effect (NHSE), where a macroscopic number of eigenstates become localized at system's boundaries [21–46]. Importantly, the non-Hermitian skin effect can exhibit either exponential or algebraic localization, depending on spatial dimensionality and other factors [24,39,47,48]. Although the non-Hermitian skin effect typically requires fully open boundaries, a single impurity that weakly breaks translational invariance can still exhibit localization behavior related to the skin effect. These key factors lead to the emergence of algebraic states in continuum (AICs) in non-Hermitian systems, which are fundamentally distinct from BICs in Hermitian systems.

We first analytically investigate the emergence of AICs in a two-dimensional continuum model with a delta-function impurity potential. Our analysis shows that the appearance of AICs requires only that the system's Bloch spectrum spans a finite area in the complex-energy plane, indicating that AICs are a generic feature of non-Hermitian systems, without the need for fine-tuning. We further demonstrate that AICs can arise in periodic-boundary lattice systems in the thermodynamic limit and derive the threshold condition for the impurity strength required to induce them. Beyond these isolated AIC states, we find that the continuum states are modified into a coherent superposition of plane waves and AIC components. Additionally, a pronounced peak in the local density of states (LDOS) appears at the AIC energy, exhibiting a resonancelike feature reminiscent of Hermitian systems.

*Contact author: cfang@iphy.ac.cn

Here we emphasize how AICs differ from other localization phenomena. In Hermitian 2D media, a point scatterer generates an outgoing cylindrical wave with envelope $|\psi_{sc}| \sim r^{-1/2}$; this follows from flux conservation (constant $2\pi r j_r$) or, equivalently, from the Hankel and stationary-phase asymptotics of integrating over the one-dimensional constant-energy contour [49]. By contrast, in our non-Hermitian setting where the Bloch spectrum covers a finite area in the complex-energy plane, a single impurity yields AICs whose envelope is algebraically localized, with the form of $|\psi| \sim r^{-1}$. The change of exponent is tied to k-space geometry: the non-Hermiticity reduces the constant-energy manifold from a 1D curve to isolated points.

Moreover, while both NHSE and AICs depend on the same bulk criterion, i.e., a finite spectral area under periodic boundary conditions (PBC) [21], AICs are nontopological in nature. AICs require neither point-gap topology nor dislocations, remain $O(1)$ in number, and display the characteristic r^{-1} profile. Thus AICs are fundamentally different from other topologically originated localization phenomena in non-Hermitian systems. For example, the dislocation induced non-Hermitian skin effect [50–54], which is a topological response of point-gapped bands, is triggered when the Burgers-vector line $B \cdot k = \pi$ winds nontrivially, and produces $O(L)$ exponentially localized modes at the dislocation core(s).

Algebraic states in continuum with a delta-type potential—Consider a two-dimensional non-Hermitian Hamiltonian $H_0(-i\partial_x, -i\partial_y)$ with a delta-function impurity potential $V = \lambda\delta(x, y)$, where $\lambda \in \mathbb{C}$ in general. The eigenvalues form a continuous spectrum in the thermodynamic limit. In Hermitian systems, a given energy E_0 inside this continuum typically corresponds to a continuum of momentum solutions: the momentum-space solution set,

$$S(E_0) \coloneqq \{\mathbf{p} | E_0 = H_0(\mathbf{p}), \mathbf{p} = (p_x, p_y) \in BZ\}, \quad (1)$$

forms a continuous contour in BZ. In contrast, for non-Hermitian systems whose spectrum spans a finite area in the complex-energy plane, $S(E_0)$ is discrete [21]. This difference in k-space structure underlies the emergence of AICs.

For simplicity, we assume that $E_0 = H_0(\mathbf{p}_0)$ is non-degenerate and take $\mathbf{p}_0 = \mathbf{0}$. A first-order expansion $H_0(\mathbf{p}) \approx E_0 + (\partial_{p_x} H_0) p_x + (\partial_{p_y} H_0) p_y$ reduces the eigenvalue equation to

$$[-i\partial_x - ia\partial_y + \tilde{\lambda}\delta(x, y)]\psi(x, y) = 0, \quad (2)$$

where $\tilde{\lambda} = \lambda / \partial_{p_x} H_0|_{\mathbf{p}=\mathbf{p}_0}$, and $a = \partial_{p_y} H_0 / \partial_{p_x} H_0|_{\mathbf{p}=\mathbf{p}_0}$ is a nonreal number. The fact that Im $a \neq 0$ means that the system's spectrum around E_0 locally occupies a finite area and vice versa. Equation (2) can be solved via Fourier transform, yielding

$$\psi(x, y) = \frac{\tilde{\lambda}\psi(0, 0)}{2\pi i} \int dk_x dk_y \frac{e^{ik_x x + ik_y y}}{k_x + ak_y}. \quad (3)$$

Without loss of generality, we assume Im $(a) > 0, x > 0, y > 0$. Evaluating Eq. (3) by residue theorem [55], we obtain

$$\psi(x, y) = \tilde{\lambda}\psi(0, 0) \frac{1}{y - ax} \propto \frac{c(\theta)}{r}. \quad (4)$$

Notably, Im $a \neq 0$ is crucial for the algebraic localization, which is guaranteed by the finite-area condition for continuum spectrum, thus making AICs unique to non-Hermitian systems in two and higher dimensions. In the Hermitian case, where $a \in \mathbb{R}$, the integral in Eq. (3) diverges, indicating the absence of such AIC solutions. This also aligns with the established theorem that BICs cannot arise in Hermitian systems with spatially confined impurity potentials [5,57]. Notably, as the system transitions from Hermitian to weak non-Hermitian, AICs emerge once the spectrum acquires any finite area, and $c(\theta)$ in Eq. (4) is controlled by Jacobian of H_0 at $\mathbf{p}_0$, i.e., $\max_\theta |c(\theta)| \propto J(\mathbf{p}_0)^{-1}$ [55].

Note that, while we focus on delta-type potentials in two dimensions here, algebraic decay is in fact a generic feature of non-Hermitian systems in dimensions $d > 1$. It arises from two ingredients: (i) the continuum spectrum occupies a finite region in the complex-energy plane, and (ii) breaking translational invariance. Both conditions remain valid in higher dimensions and for more realistic impurity potentials, provided that their tails decay sufficiently fast (e.g., screened Coulomb or Gaussian potentials). Dimensionality, however, changes the decay exponent. In the general $d > 1$ dimensional case, AICs generally decay as $r^{-(d/2)}$ with r^{-1} as an exception for specific directions. We provide a detailed derivation concerning the above points in Supplemental Material [55].

Lattice implementation and Green's function—The algebraically decaying state described above can be explicitly established in a lattice model. We consider a two-dimensional non-Hermitian tight-binding Hamiltonian H_0 with PBC, perturbed by a single on-site impurity at the origin, $\lambda|\mathbf{0}\rangle\langle\mathbf{0}|$ with $\lambda \in \mathbb{C}$. The full Hamiltonian is

$$\hat{H} = \hat{H}_0 + \lambda|\mathbf{0}\rangle\langle\mathbf{0}|, \quad \lambda \in \mathbb{C}. \quad (5)$$

Using the Green's function method [55,58,59], the eigenstate $|\psi\rangle$ with eigenvalue E_0 can be related to the Green's function $\hat{G}_0(E) = (E - \hat{H}_0)^{-1}$ as

$$\langle\mathbf{x}|\psi\rangle = \lambda\langle\mathbf{x}|(E_0 - \hat{H}_0)^{-1}|\mathbf{0}\rangle\langle\mathbf{0}|\psi\rangle. \quad (6)$$

Inserting the resolution $\mathbb{I} = \sum_{\mathbf{k} \in BZ} |\mathbf{k}\rangle\langle\mathbf{k}|$ and denoting the Bloch Hamiltonian by $H_0(\mathbf{k}) = \langle\mathbf{k}|\hat{H}_0|\mathbf{k}\rangle, \mathbf{k} = (k_x, k_y)$, we have

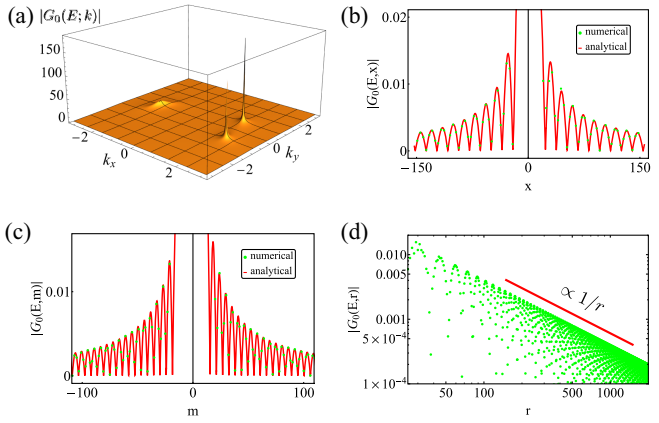

FIG. 1. AIC with $E_0 = -0.21 + 0.98i$ in model Hamiltonian $\tilde{H}_0(\mathbf{k}) = 0.6e^{ik_x} + 0.4e^{-ik_x} + 0.7ie^{ik_y} + 0.4ie^{-ik_y}$. (a) The absolute value of momentum-resolved Green's function, $|E_0 - \tilde{H}_0(\mathbf{k})|^{-1}$. The two peaks represent two momentum solutions, $\mathbf{k}_0^{(1)} \approx (1.57, 0.78), \mathbf{k}_0^{(2)} \approx (2.00, -0.76)$. The spatial profile $G_0(E, \mathbf{x})$ along the x axis in (b) and along the $x = y$ direction in (c). The green points are calculated from direct numerical integration of Eq. (7), and the red solid line is the asymptotic approximation calculated from Eq. (8) with the singularity points $\mathbf{k}_0^{(1)}, \mathbf{k}_0^{(2)}$. (d) The log-log plot of the spatial profile along the x axis.

$$G_0(E_0, \mathbf{x}) \coloneqq \langle \mathbf{x}|(E_0 - \hat{H}_0)^{-1}|\mathbf{0}\rangle = \sum_{\mathbf{k}\in BZ} \frac{\langle \mathbf{x}|\mathbf{k}\rangle\langle \mathbf{k}|\mathbf{0}\rangle}{E_0 - H_0(\mathbf{k})}. \quad (7)$$

Since the spatial profile $\psi(\mathbf{x})/(\lambda\psi(\mathbf{0}))$ corresponds directly to $G_0(E_0, \mathbf{x})$, we use these two quantities interchangeably.

We first focus on AICs and their spatial profiles. In the thermodynamic limit, the summation over $\mathbf{k}$ in Eq. (7) can be replaced by an integral [60]. In contrast to the Hermitian case, where $S(E_0)$ forms a one-dimensional contour, and the associated singularity produces scattering states, in the non-Hermitian case the set $S(E_0)$ is discrete [Fig. 1(a)] and no divergence occurs, as discussed above. These discrete momenta dominate the Green's function behavior at large $|\mathbf{x}|$. Thus, Eq. (7) can be approximated by expanding around these isolated solutions $\mathbf{k}_0 \in S(E_0)$,

$$\sum_{\mathbf{k}_0\in S(E_0)} c(\mathbf{k}_0)e^{i\mathbf{k}_0\cdot\mathbf{x}} \int d^2\mathbf{k} \frac{e^{i\mathbf{k}\cdot\mathbf{x}}}{k_x + a(\mathbf{k}_0)k_y}, \quad (8)$$

where $c(\mathbf{k}_0) = -(2\pi)^{-2}(\partial_{k_x}H_0)^{-1}|_{\mathbf{k}_0}$, and $a(\mathbf{k}_0) = (\partial_{k_y}H_0/\partial_{k_x}H_0)|_{\mathbf{k}_0}$. Each term in Eq. (8) reproduces the continuum solution for the delta impurity given by Eqs. (2) and (3), so the eigenstate is a superposition of algebraically localized components, modulated by phase factors $e^{i\mathbf{k}_0\cdot\mathbf{x}}$.

A numerical illustration is shown in Fig. 1. The model is chosen as $\tilde{H}_0(\mathbf{k}) = 0.6e^{ik_x} + 0.4e^{-ik_x} + 0.7ie^{ik_y} + 0.4ie^{-ik_y}$ with energy $E_0 = -0.21 + 0.98i$. Two discrete peaks in Fig. 1(a) correspond to two singular points, $\mathbf{k}_0^{(1)} \approx (1.57, 0.78), \mathbf{k}_0^{(2)} \approx (2.00, -0.76)$, each giving rise to an algebraically localized component, as demonstrated in Figs. 1(b) and (c). Numerical simulations (green points) show excellent agreement with the analytic results derived in Eq. (8) (solid curves). The algebraic decay of the profile can be verified in the log-log plot [Fig. 1(d)]. We emphasize that for $|\mathbf{x}| \gg 0$, the spatial profile is dominated by the singularity points, and the contribution from other detailed features, for example, the finite local maximum around $\mathbf{k}' \approx (-1.6, 0)$ in Fig. 1(a), can be neglected.

In Supplemental Material [55], we demonstrate that the same result can be derived through asymptotic analysis as $|\mathbf{x}| \to \infty$. Specifically, we present a concrete example in which the algebraic decay emerges naturally by applying standard asymptotic expansion techniques to Green's function.

Threshold eliminated by Bloch saddle point—Now that the existence of algebraic impurity states in the continuum has been established, let us investigate the impurity strength threshold required to induce such states.

Evaluating Eq. (6) at $\mathbf{x} = 0$, we define

$$f_\lambda(E) \coloneqq \lambda^{-1} - G_0(E, \mathbf{0}), \quad (9)$$

and denote $P(\lambda) = \{E|f_\lambda(E) = 0\}$. It follows that an AIC with energy E_0 is excited by an impurity with strength λ only when $E_0 \in P(\lambda)$, and its spatial profile is given by Eq. (8). Thus, the number of AICs excited is given by the cardinality of $P(\lambda)$, which is $O(1)$. Furthermore, this requirement defines a function relating the impurity strength λ and the energy E of AIC, i.e., $\lambda(E) = G_0(E, \mathbf{0})^{-1}$, with E in the continuum spectrum of $\hat{H}_0$.

Since $G_0(E, \mathbf{0})$ is continuous for E in the continuum band, $\lambda(E)$ is also continuous there [61]. Consequently, the image set, $\{\lambda(E)|E = H_0(\mathbf{k}), \mathbf{k} \in BZ\}$, forms a connected region in the complex plane. Physically, for a given system, only an impurity with strength λ inside the image set of $\lambda(E)$ can generate an AIC.

Thus, if the image set of $\lambda(E)$ covers the origin, i.e., $\lambda(E_c) = 0$, or equivalently, the integral for $G_0(E_c, \mathbf{0})$ diverges, for some E_c, no threshold impurity strength is required. Otherwise, there exists a finite threshold strength, explicitly given by $\min_{\mathbf{k}} |\lambda(H_0(\mathbf{k}))|$, necessary to induce the algebraically localized states.

As discussed above, the integral defining $G_0(E, \mathbf{0})$ is convergent if the gradient of $H_0(\mathbf{k})$, $\nabla H_0(\mathbf{k})$, is nonzero for all $\mathbf{k}$ [62]. Conversely, Ref. [59] demonstrates that the integral diverges at the Bloch saddle point [BSP, $\mathbf{k}_c$ such that $\nabla H_0(\mathbf{k}_c) = 0$] if BSP exists [63].

Physically, this implies that a finite impurity threshold is required to induce algebraically localized states if and only if the group velocity, $\nabla H_0(\mathbf{k})$, is nonzero everywhere in the Brillouin zone.

AIC as scattering wavefunction—In the Hermitian case, resonance provides a route to obtain localized, but unstable,

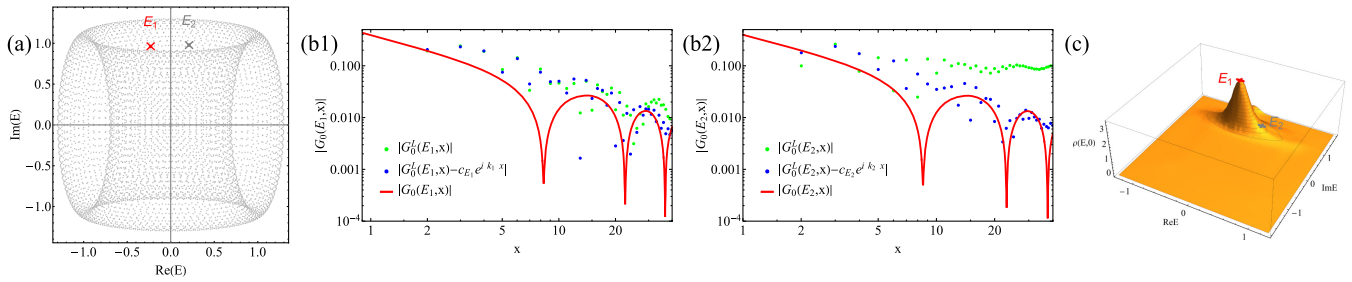

FIG. 2. (a) Perturbed spectrum of $\tilde{H}_0$ under a 80×80 lattice with impurity λ_0. The parameter is same as Fig. 1. Red cross (E_1) is the nearest eigenstate to E_0, and gray cross (E_2) is an arbitrary state. Note that a bound state [59] with energy $E_b \approx -0.22 + 2.00i$ is not shown in the figure, since it is not our focus here. (b1)[(b2)] Green dots: the spatial profile of $G_0^L(E_1, \mathbf{x})[G_0^L(E_2, \mathbf{x})]$ along the x axis; blue dots: the spatial profile subtracted by the extended plane wave part; red solid line: the asymptotic approximation of the algebraic decay calculated from Eq. (8). (c) The LDOS $\rho(E, \mathbf{0})$ of the system, with red cross and gray cross indicating the energy of E_1 and E_2, respectively.

scattering states in the continuum spectrum [1]. Similarly, in non-Hermitian systems, the general solution of the eigenvalue problem for the Hamiltonian in Eq. (5) can be expressed as

$$|\psi_{\mathbf{k}}\rangle = |\mathbf{k}\rangle + (E - \hat{H}_0)^{-1}\hat{V}|\psi_{\mathbf{k}}\rangle, \tag{10}$$

where $|\mathbf{k}\rangle$ is a plane wave with eigenvalue E. Here, we omit $\pm i0^+$ prescription in Green's function that distinguishes ingoing and outgoing limits in Hermitian scattering. More precisely, in higher-dimensional non-Hermitian systems with area-type spectrum, the elements of Green's function in position space are well defined, i.e., $\langle \mathbf{r}|(E - \hat{H}_0)^{-1}|\mathbf{r}'\rangle$ is finite and decays algebraically as $|\mathbf{r} - \mathbf{r}'|^{-1}$ for all $\mathbf{r}, \mathbf{r}'$ and E within the continuum spectrum, as shown above. Physically, $\pm i0^+$ can be understood as the on-shell constraint during the scattering process via the Sokhotski-Plemelj formula [49,55]. In the non-Hermitian case, this on-shell constraint no longer holds in the absence of energy conservation.

For each plane wave $|\mathbf{k}\rangle$, Eq. (10) defines a corresponding solution $|\psi_{\mathbf{k}}\rangle$, thus it describes all continuum states of perturbed system $\hat{H}$ [55]. Furthermore, by specifying $\hat{V} = \lambda|\mathbf{0}\rangle\langle\mathbf{0}|$ in Eq. (10) and evaluating it with $\langle \mathbf{x} = \mathbf{0}|$, one gets $\lambda\psi_{\mathbf{k}}(\mathbf{0})f_\lambda(E) = \langle \mathbf{0}|\mathbf{k}\rangle$. And thus Eq. (10) can be reduced into

$$|\psi_{\mathbf{k}}\rangle = \lambda\psi_{\mathbf{k}}(\mathbf{0})\left(f_\lambda(E)\frac{|\mathbf{k}\rangle}{\langle \mathbf{0}|\mathbf{k}\rangle} + \hat{G}_0(E)|\mathbf{0}\rangle\right). \tag{11}$$

Once one recognizes $|AIC\rangle = \hat{G}_0(E)|\mathbf{0}\rangle$ as the AIC part, one can show that all states in the continuum spectrum can be written as a superposition of the plane wave part and the AIC part. And there are specific states with energy E such that $f_\lambda(E) = 0$, i.e, no plane wave part and fully algebraically localized. Those specific states are exactly AICs as we discuss in previous Sections. In Supplemental Material [55], we provide a more detailed discussion of the finite lattice case.

In Fig. 2, an illustration of the structure of perturbed bulk eigenstates is presented. Figure 2(a) shows the spectrum of $\tilde{H}_0$ on an 80×80 lattice with impurity $\lambda_0 = G_0(E_0, \mathbf{0})^{-1} \approx -0.20 + 2.04i$, corresponding to AIC at E_0 in the thermodynamic limit. We focus on the spatial profile of the eigenstate closest to E_0, labeled E_1 (red cross), and another arbitrarily chosen state E_2 (gray cross). Since E_1 is close to E_0, its plane wave component is negligible, and the spatial profile is dominated by the algebraically localized component. In contrast, E_2 exhibits a significant plane wave component. Quantitatively, Figs. 2(b1) and 2(b2) show the spatial profile of E_1 and E_2 along the x axis (indicated by green dots), respectively. After the subtraction of the plane wave component (blue dots), the remaining term can be well approximated by AIC calculated in Eq. (8) (red solid line).

LDOS peak at AIC energy—In Hermitian systems, a characteristic signature of a resonance is a peak in the LDOS at the impurity site [49]. The LDOS at the impurity 0 is defined as the density of states weighted by the wave function amplitude at the impurity,

$$\rho(E, \mathbf{0}) \coloneqq \sum_i \delta(E - E_i)|\psi_i(\mathbf{0})|^2. \tag{12}$$

In non-Hermitian systems, the extension of this definition is not unique, since one may choose the weight to be the amplitude of the left, right, or biorthogonal eigenstates. As we shall see, however, this choice does not affect the qualitative conclusions below. For definiteness, we use the right-eigenstate weight $|\psi_i^R(\mathbf{0})|^2$.

In non-Hermitian systems, there is also a peak at the AIC energy for $\rho(E, \mathbf{0})$. For generic continuum energies, the corresponding eigenstate is a superposition of a localized (AIC-like) component and a plane-wave component, with the latter vanishing exactly at the AIC energy. Since the plane-wave part generally reduces the weight at the impurity site by delocalizing the wave function, states

with energies near the AIC energy carry larger weight than typical continuum states. Consequently LDOS develops a peak at the AIC energy. As a demonstration, Fig. 2(c) shows the LDOS at the impurity site for the model, with a pronounced peak located at E_0.

Direct *in situ* measurement of the LDOS at a complex eigenenergy is indeed challenging, especially in quantum platforms, because standard local probes access the response only at real excitation frequencies. However, the LDOS and the AIC wave function can be inferred indirectly by reconstructing the Green's function from real-frequency measurements. This type of Green's-function tomography has already been implemented in higher-dimensional acoustic lattices, where complex spectra and biorthogonal eigenmodes are extracted directly from experiment [64].

Discussions and conclusions—Since the number of AICs, i.e., the cardinality of $P(\lambda)$, is of order one, they constitute only a negligible fraction of the system's total degrees of freedom. One might question their experimental accessibility. This issue can be addressed using a perturbative approach: for a generic continuum eigenstate, one can compare its spatial profile with and without the impurity. This difference is expected to exhibit algebraic decay in space, indicating a clear experimental signature.

As a final remark, although we focus on PBC throughout, the concept of AICs can be extended to extended to open boundary conditions (OBC) [55]. Specifically, for systems with corner skin effect [48,65–68], algebraically modified states also exist in the sense that they correspond to solutions of $f_\lambda(E) = 0$ within the continuum spectrum. Intuitively, with the exponential suppression of skin effect, such states generally behave as $O(|\mathbf{r} - \mathbf{r}_{\text{imp}}|^{-1} e^{-\boldsymbol{\mu}\cdot\mathbf{r}})$ with $\mathbf{r}_{\text{imp}}$ as the position of the impurity. For systems with algebraic skin effect [48], the generalization of AICs is subtle since biorthogonal decomposition is challenging in this case. We conjecture that AICs are still greatly suppressed and hard to observe as suggested by numerics [55], given that skin modes are rather robust against local perturbation.

We emphasize that in non-Hermitian systems where the skin effect is absent under specific open boundary geometries—for example, systems exhibiting geometry-dependent skin effects [21,69–74]—the AICs behave analogously to the PBC case and thus remain observable. Moreover, this class of systems is known to generically host Bloch saddle points [59], implying that even infinitesimal impurity potential is sufficient to induce algebraically localized states embedded in the continuum spectrum.

Acknowledgments—We thank Zixi Fang for helpful discussions. C. F. acknowledges funding support by National Natural Science Foundation of China (NSFC) under Grants No. 12325404, No. 12547112, and No. 12188101, and National Key R&D Program of China under Grants No. 2022YFA1403800 and No. 2023YFA1406704.

Data availability—The data that support the findings of this article are not publicly available because they contain sensitive personal information. The data are available from the authors upon reasonable request.

[1] P. Phillips, *Advanced Solid State Physics* (Cambridge University Press, Cambridge, England, 2012).
[2] P. W. Anderson, Phys. Rev. **109**, 1492 (1958).
[3] F. Evers and A. D. Mirlin, Rev. Mod. Phys. **80**, 1355 (2008).
[4] J. B. Conway, *A Course in Functional Analysis* (Springer, New York, 2019), Vol. 96.
[5] C. W. Hsu, B. Zhen, A. D. Stone, J. D. Joannopoulos, and M. Soljačić, Nat. Rev. Mater. **1**, 16048 (2016).
[6] I. Rotter, J. Phys. A **42**, 153001 (2009).
[7] S. Diehl, E. Rico, M. A. Baranov, and P. Zoller, Nat. Phys. **7**, 971 (2011).
[8] S. Malzard, C. Poli, and H. Schomerus, Phys. Rev. Lett. **115**, 200402 (2015).
[9] J. Dalibard, Y. Castin, and K. Mølmer, Phys. Rev. Lett. **68**, 580 (1992).
[10] A. Regensburger, C. Bersch, M.-A. Miri, G. Onishchukov, D. N. Christodoulides, and U. Peschel, Nature (London) **488**, 167 (2012).
[11] T. Gao, E. Estrecho, K. Y. Bliokh, T. C. H. Liew, M. D. Fraser, S. Brodbeck, M. Kamp, C. Schneider, S. Höfling, Y. Yamamoto, F. Nori, Y. S. Kivshar, A. G. Truscott, R. G. Dall, and E. A. Ostrovskaya, Nature (London) **526**, 554 (2015).
[12] L. Feng, R. El-Ganainy, and L. Ge, Nat. Photonics **11**, 752 (2017).
[13] R. El-Ganainy, K. G. Makris, M. Khajavikhan, Z. H. Musslimani, S. Rotter, and D. N. Christodoulides, Nat. Phys. **14**, 11 (2018).
[14] M.-A. Miri and A. Alù, Science **363**, eaar7709 (2019).
[15] Ş. K. Özdemir, S. Rotter, F. Nori, and L. Yang, Nat. Mater. **18**, 783 (2019).
[16] V. Kozii and L. Fu, Phys. Rev. B **109**, 235139 (2024).
[17] H. Shen and L. Fu, Phys. Rev. Lett. **121**, 026403 (2018).
[18] Y. Nagai, Y. Qi, H. Isobe, V. Kozii, and L. Fu, Phys. Rev. Lett. **125**, 227204 (2020).
[19] F. Song, S. Yao, and Z. Wang, Phys. Rev. Lett. **123**, 170401 (2019).
[20] Y. Ashida, Z. Gong, and M. Ueda, Adv. Phys. **69**, 249 (2020).
[21] K. Zhang, Z. Yang, and C. Fang, Nat. Commun. **13**, 2496 (2022).
[22] T. E. Lee, Phys. Rev. Lett. **116**, 133903 (2016).
[23] V. M. Martinez Alvarez, J. E. Barrios Vargas, and L. E. F. Foa Torres, Phys. Rev. B **97**, 121401(R) (2018).
[24] S. Yao and Z. Wang, Phys. Rev. Lett. **121**, 086803 (2018).
[25] F. K. Kunst, E. Edvardsson, J. C. Budich, and E. J. Bergholtz, Phys. Rev. Lett. **121**, 026808 (2018).
[26] S. Yao, F. Song, and Z. Wang, Phys. Rev. Lett. **121**, 136802 (2018).
[27] K. Yokomizo and S. Murakami, Phys. Rev. Lett. **123**, 066404 (2019).
[28] C. H. Lee and R. Thomale, Phys. Rev. B **99**, 201103(R) (2019).

[29] C. H. Lee, L. Li, and J. Gong, Phys. Rev. Lett. **123**, 016805 (2019).
[30] S. Longhi, Phys. Rev. Res. **1**, 023013 (2019).
[31] K. Zhang, Z. Yang, and C. Fang, Phys. Rev. Lett. **125**, 126402 (2020).
[32] N. Okuma, K. Kawabata, K. Shiozaki, and M. Sato, Phys. Rev. Lett. **124**, 086801 (2020).
[33] D. S. Borgnia, A. J. Kruchkov, and R.-J. Slager, Phys. Rev. Lett. **124**, 056802 (2020).
[34] Z. Yang, K. Zhang, C. Fang, and J. Hu, Phys. Rev. Lett. **125**, 226402 (2020).
[35] Y. Yi and Z. Yang, Phys. Rev. Lett. **125**, 186802 (2020).
[36] L. Xiao, T. Deng, K. Wang, G. Zhu, Z. Wang, W. Yi, and P. Xue, Nat. Phys. **16**, 761 (2020).
[37] A. Ghatak, M. Brandenbourger, J. van Wezel, and C. Coulais, Proc. Natl. Acad. Sci. U.S.A. **117**, 29561 (2020).
[38] T. Helbig, T. Hofmann, S. Imhof, M. Abdelghany, T. Kiessling, L. W. Molenkamp, C. H. Lee, A. Szameit, M. Greiter, and R. Thomale, Nat. Phys. **16**, 747 (2020).
[39] L. Li, C. H. Lee, S. Mu, and J. Gong, Nat. Commun. **11**, 5491 (2020).
[40] K. Kawabata, N. Okuma, and M. Sato, Phys. Rev. B **101**, 195147 (2020).
[41] C. C. Wanjura, M. Brunelli, and A. Nunnenkamp, Nat. Commun. **11**, 3149 (2020).
[42] W.-T. Xue, M.-R. Li, Y.-M. Hu, F. Song, and Z. Wang, Phys. Rev. B **103**, L241408 (2021).
[43] L. Li, S. Mu, C. H. Lee, and J. Gong, Nat. Commun. **12**, 5294 (2021).
[44] K. Zhang, C. Fang, and Z. Yang, Phys. Rev. Lett. **131**, 036402 (2023).
[45] S. Longhi, Phys. Rev. Lett. **128**, 157601 (2022).
[46] Y.-M. Hu, H.-Y. Wang, Z. Wang, and F. Song, Phys. Rev. Lett. **132**, 050402 (2024).
[47] K. Kawabata, T. Numasawa, and S. Ryu, Phys. Rev. X **13**, 021007 (2023).
[48] K. Zhang, C. Shu, and K. Sun, Phys. Rev. X **15**, 031039 (2025).
[49] E. N. Economou, *Green's Functions in Quantum Physics* (Springer Science & Business Media, New York, 2006), Vol. 7.
[50] F. Schindler and A. Prem, Phys. Rev. B **104**, L161106 (2021).
[51] B. A. Bhargava, I. C. Fulga, J. Van Den Brink, and A. G. Moghaddam, Phys. Rev. B **104**, L241402 (2021).
[52] A. Panigrahi, R. Moessner, and B. Roy, Phys. Rev. B **106**, L041302 (2022).
[53] H. Xue, D. Jia, Y. Ge, Y. J. Guan, Q. Wang, S. Q. Yuan, H. X. Sun, Y. D. Chong, and B. Zhang, Phys. Rev. Lett. **127**, 214301 (2021).
[54] W. Wu, Q. Zhang, L. Qi, K. Zhang, S. Tong, and C. Qiu, Adv. Mater. **38**, e14101 (2026).
[55] See Supplemental Material at http://link.aps.org/supplemental/10.1103/9dhm-k5kf for more details, which includes Ref. [56].
[56] P. D. Miller, *Applied Asymptotic Analysis* (American Mathematical Society, Providence, 2006), Vol. 75.
[57] J. von Neumann and E. P. Wigner, *The Collected Works of Eugene Paul Wigner: Part A: The Scientific Papers* (Springer, Berlin, Heidelberg, 1993), p. 291.
[58] Z. Fang, C. Fang, and K. Zhang, Phys. Rev. B **108**, 165132 (2023).
[59] A. Yang, Z. Fang, K. Zhang, and C. Fang, Commun. Phys. **8**, 124 (2025).
[60] The theory for bound state with energy outside the continuum spectrum has been established in Refs [58,59].
[61] As a side remark, $\lambda(E)$ is in fact nonanalytic. Since the singularity set depends on E nonanalytically, $\lambda^{-1}(E)$ also exhibits nonanalytic behavior [55].
[62] Technically, what we have shown applies to a system whose gradient is nonzero. Thus, to complete the proof of this statement, one needs to prove the convergence of integral if the integrand near the singularity behaves like $(1/k_x^n + ak_y), a \in \mathbb{C}\backslash\mathbb{R}, n \geq 2$. We omit the mixing term $k_x^{n-m}k_y^m$ here since one can extract the common k_y as $k_y(a + O(k))$ which is dominated by k_y near the origin. To show the convergence, one just needs to apply the residue theorem to integrate out k_x and gets $\int k_y(k_y)^{[1-n/n]}$, which is convergent.
[63] We remark that Ref. [59] deals with bound states outside the spectrum, i.e., $\lambda(E)$ for $E \in \mathbb{C}\backslash\{H_0(\mathbf{k}), \mathbf{k} \in BZ\}$. By Liouville's theorem, this function takes the minimum value at the boundary. So BSP needs to be at the boundary of the spectrum to eliminate the threshold. Since we are now considering states in the continuum, this constraint can be relaxed.
[64] J.-X. Zhong, J. Kim, K. Chen, J. Lu, K. Ding, and Y. Jing, Phys. Rev. B **112**, L220301 (2025).
[65] H.-Y. Wang, F. Song, and Z. Wang, Phys. Rev. X **14**, 021011 (2024).
[66] K. Zhang, Z. Yang, and K. Sun, Phys. Rev. B **109**, 165127 (2024).
[67] Z. Xu, B. Pang, K. Zhang, and Z. Yang, arXiv:2311.16868.
[68] Y. Xiong, Z.-Y. Xing, and H. Hu, arXiv:2407.01296.
[69] Y.-C. Wang, J.-S. You, and H. H. Jen, Nat. Commun. **13**, 4598 (2022).
[70] Q. Zhou, J. Wu, Z. Pu, J. Lu, X. Huang, W. Deng, M. Ke, and Z. Liu, Nat. Commun. **14**, 4569 (2023).
[71] W. Wang, M. Hu, X. Wang, G. Ma, and K. Ding, Phys. Rev. Lett. **131**, 207201 (2023).
[72] T. Wan, K. Zhang, J. Li, Z. Yang, and Z. Yang, Sci. Bull. **68**, 2330 (2023).
[73] Y. Qin, K. Zhang, and L. Li, Phys. Rev. A **109**, 023317 (2024).
[74] E. Zhao, Z. Wang, C. He, T. F. J. Poon, K. K. Pak, Y.-J. Liu, P. Ren, X.-J. Liu, and G.-B. Jo, Nature (London) **637**, 565 (2025).